Time-Resolved X-Ray Diffraction by Skinned Skeletal Muscle Fibers during Activation and Shortening

B. K. Hoskins,* C. C. Ashley,* G. Rapp,† and P. J. Griffiths*
*University Laboratory of Physiology, Oxford OX1 3PT, United Kingdom; and †EMBL Outstation, 22603 Hamburg, Germany

ABSTRACT Force, sarcomere length, and equatorial x-ray reflections (using synchrotron radiation) were studied in chemically skinned bundles of fibers from *Rana temporaria* sartorius muscle, activated by UV flash photolysis of a new photolabile calcium chelator, NP-EGTA. Experiments were performed with or without compression by 3% dextran at 4°C. Isometric tension developed at a similar rate ($t_{1/2} = 40 \pm 5$ ms) to the development of tetanic tension measured in other studies (Cecchi et al., 1991). Changes in intensity of equatorial reflections (I_{11} $t_{1/2}$, 15–19 ms; I_{10} $t_{1/2}$, 24–26 ms) led isometric tension development and were faster than for tetanus. During shortening at $0.14P_o$, I_{10} and I_{11} changes were partially reversed (18% and 30%, respectively, compressed lattice), in agreement with intact cell data. In zero dextran, activation caused a compression of A-band lattice spacing by 0.7 nm. In 3% dextran, activation caused an expansion of 1.4 nm, consistent with an equilibrium spacing of 45 nm. But, in both cases, discharge of isometric tension by shortening caused a rapid lattice expansion of 1.0–1.1 nm, suggesting discharge of a compressive cross-bridge force, with or without compression by dextran, and the development of an additional expansive force during activation. In contrast to I_{10} and I_{11} data, these findings for lattice spacing did not resemble intact fiber data.

INTRODUCTION

Although the physiological, structural, and biochemical characteristics of whole muscle have been well documented, and considerable recent progress has been made in the understanding of the structure and interaction of isolated contractile proteins (Highsmith, 1999; Molloy et al., 1995), there remains uncertainty about the activation and tension-generating processes in skeletal muscle at the molecular level within the intact myofilament lattice, where interaction between myofilament proteins and structural constraints can modulate the molecular events observed in isolated proteins. X-ray diffraction provides a powerful, noninvasive technique for studying structural changes of the contractile system in situ, while maintaining the integrity of lattice structure.

Currently it is thought that the myosin moiety, S1, binds to the thin filament and undergoes a force-generating distortion (the power stroke). Crystal structures of different allosteric states of the cross-bridge cycle (Highsmith, 1999) show a change in the orientation of the S1 tail element, consistent with the proposal that rotation of this region of S1 is the power stroke distortion (Huxley, 1969; Huxley and Kress, 1985; Tokunaga et al., 1987). Orientational studies of the S1 tail in the intact myofilament lattice, using spin labels or fluorescence polarization, also suggest rotation of this region between pre- and post-power stroke states (Brust-Mascher et al., 1999; Corrie et al., 1999). S1 binding to actin and the subsequent power stroke produce an altered mass distribution within the myofilament lattice, affecting the intensities and positions of reflections in the muscle x-ray diffraction pattern. With the development of synchrotron radiation sources and fast electronic detectors, time-resolved studies of these physical changes by x-ray diffraction became possible and have been performed on whole muscle (Huxley et al., 1981), and more recently on single intact muscle fibers (Cecchi et al., 1990).

Skinned muscle fibers, where the sarcolemma has been disrupted by chemical or mechanical means, permit direct control of the immediate chemical environment of the contractile proteins, thus avoiding changes in excitation-contraction coupling and membrane excitability, which may occur during electrical stimulation of intact cells. But activation of skinned fibers by diffusion of externally applied calcium is slow, and they usually sustain only brief periods of maximal tension generation before severe sarcomere disordering and disruption of the x-ray pattern occur. Recently, photolabile calcium chelators have been developed, from which calcium ions are rapidly liberated following a pulse of UV radiation, permitting activation of skinned fibers without appreciable diffusional delays or prolonged tension generation. Here we report x-ray diffraction studies performed with a new photolabile calcium chelator, *o*-nitrophenyl EGTA (NP-EGTA) (Ellis-Davies and Kaplan, 1994), which has important advantages over earlier forms of caged calcium. This method of activation also permitted us to obtain time-resolved x-ray diffraction measurements on skinned fibers under isotonic conditions for the first time, as shortening can be imposed within 400 ms of activation, while the condition of the preparation remains good.

Cross-bridge activity causes both a changed A-band mass distribution and development of a radial force (evident as a compression of the A-band lattice) (Maughan and Godt, 1981; Matsubara et al., 1984; Brenner and Yu, 1991). The dynamic properties of this radial force have been studied

Received for publication 20 April 2000 and in final form 11 October 2000.
Address reprint requests to Dr. P.J. Griffiths, University Laboratory of Physiology, Parks Road, Oxford OX1 3PT, UK. Tel.: 44-1865-272494; Fax: 44-1865-272469; E-mail: pjg@physiol.ox.ac.uk.

0006-3495/01/01/398/17 $2.00

only in intact cells (Cecchi et al., 1990; Bagni et al., 1994; Irving et al., 1998; Ashley et al., 1999). The force required to compress an intact muscle fiber is large, as it must overcome the osmotic pressure difference produced across the sarcolemma as the sarcoplasm becomes more concentrated; hence relaxed intact cells maintain a constant volume at different sarcomere lengths (Elliott et al., 1963; Matsubara and Elliott, 1972). Consequently, lattice spacing changes accompanying active sarcomere shortening of intact cells may include constant volume effects. This was thought not the case with skinned fibers (Matsubara and Elliott, 1972; Matsubara et al., 1984). Hoskins et al. (1999) recently investigated dynamic spacing changes in skinned fibers following a change in axial load at sub-millisecond time resolution, but only in low-force states or relaxation, so as to minimize preparation deterioration. Here we present dynamic spacing measurements associated with changes in axial load from skinned fibers in the activated state, obtained by performing changes in load immediately after peak tension was attained, following NP-EGTA flash activation.

MATERIALS AND METHODS

Preparations

One to three cut end fibers were dissected from sartorius muscle of *Rana temporaria* and mounted on titanium hooks, attached to a force transducer and a moving coil stretcher motor (Hoskins et al., 1999). In early experiments, fibers were mounted using aluminum clips, but passage of the fiber through the solution meniscus before flashing caused vertical displacement out of the laser beam used for sarcomere length measurement, which was focused to a 250-μm spot, due to small displacements of the clips about the titanium hooks. Subsequently we attached preparations to the hooks by cyanoacrylate glue, which reduced this vertical displacement problem. Fibers were then transferred to a skinning solution (1% v/v Triton X-100) for 2 min to disrupt the sarcolemma, using a rotating chamber system (Auden Scientific Instruments, Abingdon, UK) described in detail in Griffiths and Jones (1994) and Hoskins et al. (1999). This duration of skinning was found to be sufficient to render the membrane permeable while minimizing disorder within the fiber lattice (Hoskins et al., 1999). Experimental chambers were 1-mm-wide slits in aluminum blocks with Kapton (Goodfellow Cambridge, Cambridge, UK) walls, containing 70 μl of solution, maintained at 5°C by perfusion of a cooling block below the chamber base. Fibers were mounted horizontally with the synchrotron radiation beam directed perpendicular to the fiber axis (beam dimensions, 0.3×4 mm, $\lambda = 0.15$ nm). A diode laser beam ($\lambda = 680$ nm) was directed through the preparation at an angle to the horizontal plane, to avoid obstruction of the x-ray beam by the diffracted laser beam position detector electronics.

Solutions

To avoid damage and disordering brought about by the long exposure required for activation by a $[Ca^{2+}]$ change in the bulk bathing medium, we activated our preparations by photolysis of caged calcium in air. The photolabile calcium chelator NP-EGTA was selected as the caged calcium for these experiments, as the large change in Ca^{2+} affinity upon photolysis (12,500-fold) (Ellis-Davies and Kaplan, 1994) permitted abrupt changes in free calcium concentration, $[Ca^{2+}]$, across the fiber cross section. The magnesium affinity of NP-EGTA is low ($K_d = 9.0$mM) (Ellis-Davies and Kaplan, 1994) and does not change significantly upon photolysis.

Experiments were performed with and without 3% dextran T500 in the bathing solution to investigate the dependence of the changes in the equatorial x-ray diffraction pattern on the initial lattice spacing. Godt and Maughan (1981) showed that 3–5% dextran T500 compressed single skinned fibers to their in vivo diameter, and our lattice spacing measurements confirmed this.

Solutions were adjusted to pH 7.0, 200 mM ionic strength, and were calculated to contain 1 mM $[Mg^{2+}]$ at 5°C, using an iterative method developed from Perrin and Sayce (1967). The fibers were exposed to a zero EGTA washing solution, before transfer to the caged calcium loading solution, to wash out residual EGTA, which would otherwise compete with NP-EGTA to bind calcium. Solution compositions were as follows: relaxing solution, 20 mM *N*,*N*-bis[2-hydroxyethyl]-2-aminoethanesulfonic acid (BES), 10 mM EGTA, 5 mM Na_2ATP, 5.6 mM $MgCl_2$, 37.4 mM KOH, 62.1 mM potassium propionate, 20 U/ml phosphocreatine phosphokinase, and 10 mM creatine phosphate; zero EGTA washing solution, 50 mM BES, 5 mM Na_2ATP, 5.6 mM $MgCl_2$, 12 mM KOH, 88 mM potassium propionate, 20 U/ml creatine phosphokinase, and 10 mM creatine phosphate; loading solution, as washing solution plus 2.84 mM NP-EGTA, and 1.36 mM $CaCl_2$. Dextran T500 (3%) was added to all solutions for experiments performed at a compressed lattice spacing.

Experimental protocol

Preparations were equilibrated in washing solution for 5 min and then in loading solution for another 5 min. During the period in washing solution, fiber position was optimized during exposure to a 90% attenuated x-ray beam. Because the fiber scattered more strongly than the bathing solution or the chamber windows, total detector counts were maximized by vertical displacement of the entire experimental setup in 10-μm steps. After loading, fibers were flashed in air with a UV pulse from the xenon flash lamp (Rapp Optoelektronik, Hamburg, Germany) to photolyze the caged calcium. To minimize the period of high tension development, fibers were transferred to relaxing solution within 1.5 s of the initial flash. The x-ray shutter (opening time, 5 ms) was triggered 150 ms before the flash to obtain baseline relaxed data and closed within 1 s afterwards. As a result of exposing the fiber in air, intensities of reflections increased by 24.9% compared with the intensity in the optimum beam position in relaxing solution, principally due to the loss of scattering effects from the Kapton window and saline between the fiber and the source. All time axes in subsequent figures refer to the time elapsed from the start of the sequence of timing pulses synchronizing the solution changer, shutter, stretcher, and flash lamp. The lamp light was focused by a cylindrical lens to an elliptical spot of 6 mm $\times$ 3 mm at a working distance from the lens of 18 mm, and filtered (78% transmission at 340 nm). The flash was delayed by 1 s after a pulse from the data collection system to the solution changer, which caused the fiber to be suspended above a 1-cm-deep well, which acted as a light sink. This procedure minimized photolysis of the loading solution in adjacent chambers by reflected UV light. Exposure to air, in total, was ~1.5 s. Control experiments in which the experimental procedure was repeated 10 times without exposure to either flash or synchrotron radiation showed that the preparation underwent no deterioration as a result of this protocol. However, it was rarely possible to obtain more than four activations from a given fiber without severe deterioration. Although the origin of this deterioration could not be determined precisely, it did not occur when the preparation was flashed and exposed to x-rays in the absence of caged calcium, suggesting that the development of force or the photolysis reaction was responsible. Because photolysis was incomplete for a single flash, the level of activation of fibers was tested by exposure to a second flash. If additional tension development occurred, the molar ratio of calcium to NP-EGTA in the loading solution was increased until full activation could be achieved from a single flash with minimal pre-flash activation.

In some experiments, at the isometric tension plateau between 300 and 400 ms after the flash, fibers were allowed to shorten rapidly by up to 6.7%. In the first 0.3 ms, the fiber received a step release, which was followed by 50 ms of ramp shortening, which maintained tension at a low level. Because force during shortening could not be adjusted in advance without activation of the preparation, isotonic tension varied between 0 and $0.3P_o$. The release was then maintained until the fiber had been returned to relaxing solution and tension discharged.

Data collection and processing

Equatorial x-ray diffraction patterns were recorded on beam line X-13 of the EMBL outstation (Hamburg, Germany), using a linear wire per wire detector (Hendrix et al., 1982) sampling at 5-ms time resolution. Data sets were summed to achieve a sufficiently good signal-to-noise ratio using the package OTOKO (Koch and Bendall, 1981), to allow fitting of the data to an algorithm describing the equatorial spectrum (Yu et al., 1985; Hoskins et al., 1999), from which spacing and intensity parameters were determined. Usually, a total exposure time of 10 ms (two data sets) was required, however, in exceptional cases, this was reduced to 5 ms. Tension, sarcomere length, and fiber length were also recorded simultaneously. Because of potential deterioration in sarcomere length homogeneity at full activation, even for such brief activation periods as used here, sarcomere length measurement by a position-sensing photodiode, as used in Hoskins et al. (1999), was deemed inappropriate, because this method provided no index of the quality, or even the existence, of the diffracted laser beam. We therefore changed to a scanning photodiode array system (128G, EG&G Reticon, Sunnyvale, CA). The output of each array element was integrated on sequential readout (collection period 16 ms), and the total intensity from that element was captured by a sample and hold circuit. This value was then clocked out to a digital storage oscilloscope, using gated clock pulses from the array control board to trigger data acquisition. In this way a two-dimensional image of one of the first-order diffracted laser beams could be stored for subsequent analysis for mean position and width. The relaxed sarcomere length was set to 2.2 μm at the beginning of the experiment. Sarcomere length records were not summed. The first-order sarcomere reflection contained a complex substructure of peaks, due to the varying Bragg angle subtended by different populations of sarcomeres (Zite-Ferenczy et al., 1986). During activation, peaks appeared and disappeared in different regions of the detector field, making it difficult to follow the position of a single peak throughout tension development. Instead, we calculated sarcomere length for the whole population of subpeaks within the first-order reflection, using the expected x value of the detector pattern ($\Sigma I(x_i)x_i/\Sigma I(x_i)$, where $I(x_i)$ was the intensity recorded at array element position x_i), after background subtraction by eye. We were unable to obtain sarcomere records for all fibers used in this study, due to intensity loss in the laser diffraction pattern, possibly because of a residual vertical displacement. In addition, sarcomere pattern quality was usually much reduced after the first flash activation. Nevertheless, in 17 experiments in which fibers were maintained in the laser beam, a laser diffraction pattern could be obtained throughout isometric tension development. All software for x-ray or sarcomere spectra analysis were written in Salford Fortran 77, Fortran 90, or Borland C, and numerical techniques applied were taken from Press et al. (1989).

For ease of display of intensity data, intensity changes are plotted after normalization to the intensity change between relaxation and maximum isometric tension. The relative change in 10 intensity has been inverted, causing both 10 and 11 signals to rise during activation, to permit easier comparison of time courses. Owing to the slow sampling rate and the noise present in intensity records, half times of intensity changes were not measured directly. Instead we assumed that the underlying chemical reactions were likely to follow exponential time courses, and we estimated half time from the best fit to an exponential function. Lattice spacing (a), defined here as the nearest-neighbor separation between thick filaments, was calculated from the positions of the 1,0 and 1,1 reflections (x_{10} and x_{11}, respectively), according to the relations

$$a = \frac{2\lambda l}{x_{10}\sqrt{3}} = \frac{2\lambda l}{x_{11}},$$

where λ was 0.15 nm and l was 3.5–4 m. All data quoted are means ± SE unless stated otherwise.

RESULTS

Force and sarcomere length responses

Because skinned fibers swell as a result of membrane disruption, we performed experiments both with and without 3% dextran, which osmotically compresses the skinned fiber to its in vivo volume. In the absence of dextran, flash photolysis of caged calcium caused force rapidly to rise to a maximum (P_o) of 119 ± 17 kN m^{-2} (n = 17) at 5°C. The half time ($t_{1/2}$) of tension rise was 39 ± 4 ms (n = 28), similar to values of the $t_{1/2}$ for tension rise during tetanic stimulation (38–45 ms between 4°C and 8°C (Kress et al., 1986; Cecchi et al., 1991; Bordas et al., 1993) in whole muscles and intact frog fibers). In the presence of 3% dextran, force development was not significantly altered (maximum isometric tension was 119 ± 14 kN m^{-2}; n = 12) and rose with a $t_{1/2}$ of 40 ± 5 ms, n = 10. When shortening was permitted, isometric tension redevelopment after shortening was always incomplete. In the compressed lattice (3% dextran), the mean recovered tension was 0.82 ± 0.07 P_o (mean ± SD), whereas for the uncompressed lattice (zero dextran) mean recovery was 0.46 ± 0.20 P_o (mean ± SD).

Sarcomere length was recorded simultaneously with x-ray data. Of 17 fibers (5 in dextran) in which sarcomere length could be measured during tension development, 3 experiments showed no change, 9 showed a mean decrease of 3.18 ± 0.61%, and 5 records showed a mean increase of 3.27 ± 0.83%. In a constant volume system, an increase in sarcomere length of 3.27% would lead to an A-band lattice spacing decrease of 1.6% (~0.6 nm). Shortening of sarcomere length by 3.18% would result in a 1.6% lattice expansion. Although a laser diffraction pattern could be maintained after isometric tension had plateaued, deterioration of the pattern increased with time allowed at high force. Fibers in which no sarcomere length change occurred on activation also showed no sarcomere response to a release, indicating that the laser beam was directed at a fiber region that had been fixed by cyanoacrylate exposure.

Equatorial intensity changes

The uncompressed lattice

Fig. 1 shows the equatorial x-ray diffraction patterns obtained from a single skinned muscle fiber before (Fig. 1 *A*) and after (Fig. 1 *B*) NP-EGTA photolysis, recorded during

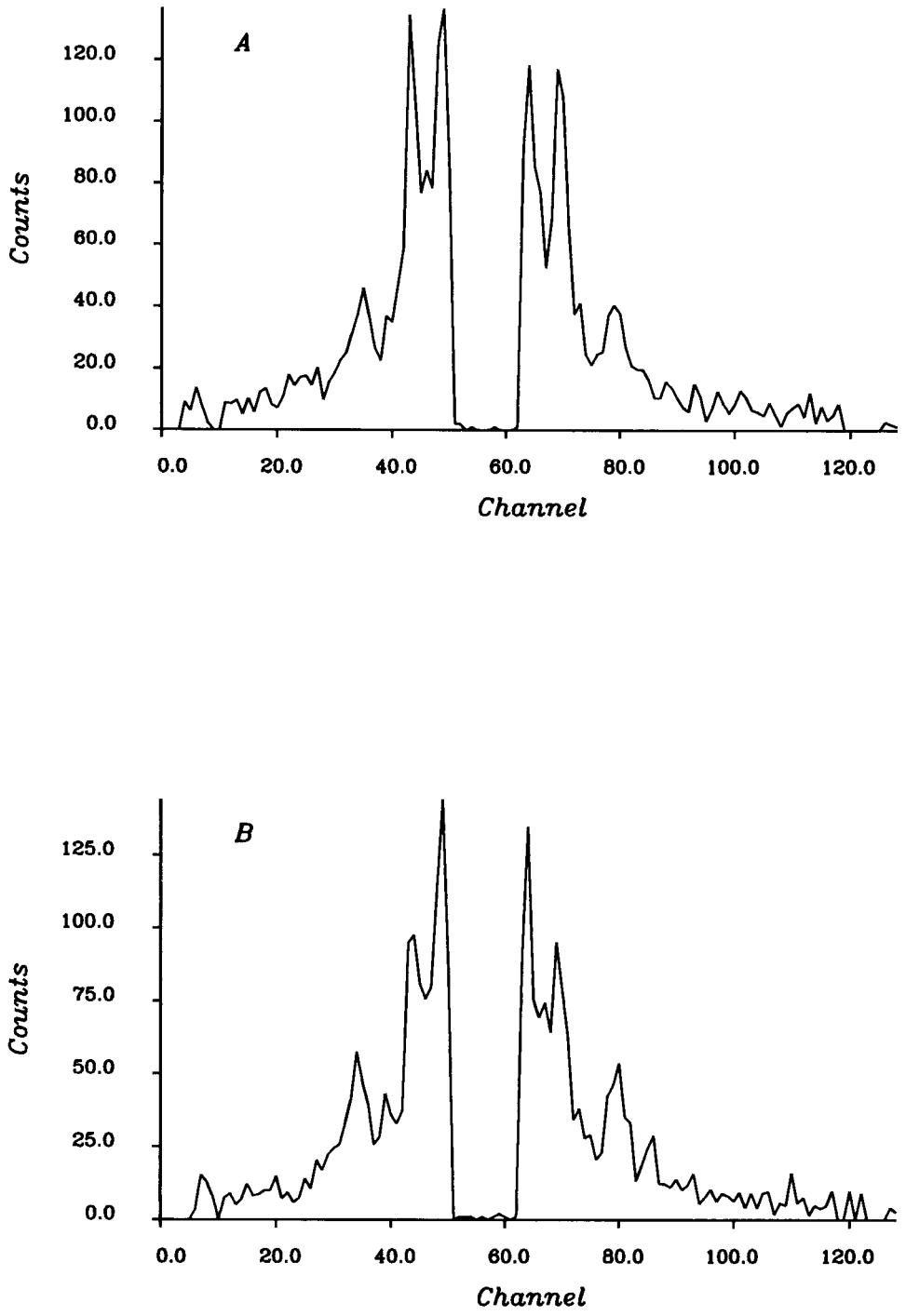

FIGURE 1 X-ray spectra from a single muscle fiber (zero dextran) in the relaxed state (*A*) and 185 ms after UV flash (*B*), when force was maximal. Both spectra were obtained in air; *B* was obtained 275 ms after *A*, and total exposure time was 10 ms for each spectrum. The spectra have been corrected for nonlinearities in the detector response by division by the normalized detector response to a uniform radiation field. Fiber number Z37 (May, 1997).

a 5-ms time-resolution experiment. Although the weaker equatorial reflections are submerged in the counting noise, both the 1,0 and 1,1 reflections are clearly discernible. Because deterioration of the preparation prevented averaging of very large numbers of activations, and hence the improvement of signal-to-noise ratios at higher time resolution, it is this consideration that ultimately limited our sampling time to 5 ms, which is a much lower time resolution than has been possible in intact fiber work (cf. Ashley et al., 1999).

Fig. 2 shows 10 and 11 intensities and force responses to NP-EGTA photolysis, averaged from nine bundles used during a single beam time to permit comparison of intensity and force time courses with minimum noise. The rise in force was accompanied by rapid changes in the equatorial 10 and 11 intensities (I_{10} and I_{11}, respectively). I_{10} decreased by 32 ± 4%, whereas I_{11} increased by 52 ± 9% ($n = 13$). Consequently, I_{11}/I_{10} increased from 0.66 ± 0.06 ($n = 13$) in the relaxed state to 1.42 ± 0.1 ($n = 13$) at the tension plateau. Where half times could be determined from individual bundles, the $t_{1/2}$ of the decrease in I_{10} was 26 ± 3 ms ($n = 30$) whereas the increase in I_{11} was more rapid ($t_{1/2} = 19 \pm 4$ ms; $n = 23$), giving a lead over tension of 13 ms and 20 ms, respectively (see Table 1).

During shortening, intensity changes were small compared with those upon activation (Fig. 3). Measurement of intensity changes during shortening was complicated by the tendency of the fiber to move in the beam and by the presence of a low level of activation in some preparations before the flash. Although we attempted to correct for fiber movement in the beam by adjusting spectra to maintain a constant total photon count throughout the data collection (as the principal source of scattered radiation was the fiber), movement was still evinced by an increase or decrease of both I_{10} and I_{11}, or a pronounced change in one reflection without alteration of the other. Data showing such behavior were eliminated from our analysis. The effect of initial activation was evident as either a fall in force during shortening below the initial tension before the flash or a change in intensity exceeding that associated with isometric activation. When fibers displaying this behavior were also excluded, we obtained an increase in I_{10} to 71.0 ± 5.8% ($n = 11$) of the intensity change associated with activation (i.e., a 29% reversal of the intensity fall that accompanied isometric activation). I_{11} decreased to 54.5 ± 6.3% ($n = 11$) of the change in intensity during activation. The mean tension during shortening was 0.141 ± 0.097 P_o (mean ± SD). Tension recovery after termination of shortening was variable (0.460 ± 0.199 P_o, mean ± SD), whereas I_{10} recovered to 110.6 ± 12.9% and I_{11} to 49.9 ± 5.6% of their initial intensity change on activation. This failure to converge on a similar recovery level suggests a possible residual movement artifact, which would cause 10 changes during shortening to be underestimated, 11 changes to be overestimated. The change in intensities was delayed with respect to the release, developing more gradually than the tension drop, in agreement with Huxley et al. (1988).

TABLE 1 The $t_{1/2}$ of changes in the force, intensities, and lattice spacing following photolysis of NP-EGTA

	Uncompressed (ms)	Compressed (3% dextran) (ms)
Force	39.0 ± 4.3 (28)	40.1 ± 5.5 (10)
I_{10}	25.9 ± 3.3* (30)	23.6 ± 2.1† (14)
I_{11}	18.9 ± 4.0† (23)	15.3 ± 3.0‡ (12)
Lattice spacing	18.2 ± 3.1‡ (10)	16.4‡ ± 3.1 (7)

Values are mean ± SE with the number of experiments in parentheses.
*Statistically faster than force; $p < 0.05$.
†Statistically faster than force; $p < 0.005$.
‡Statistically faster than force; $p < 0.001$. In the compressed lattice, I_{11} was significantly faster than I_{10} at the $p < 0.05$ level.

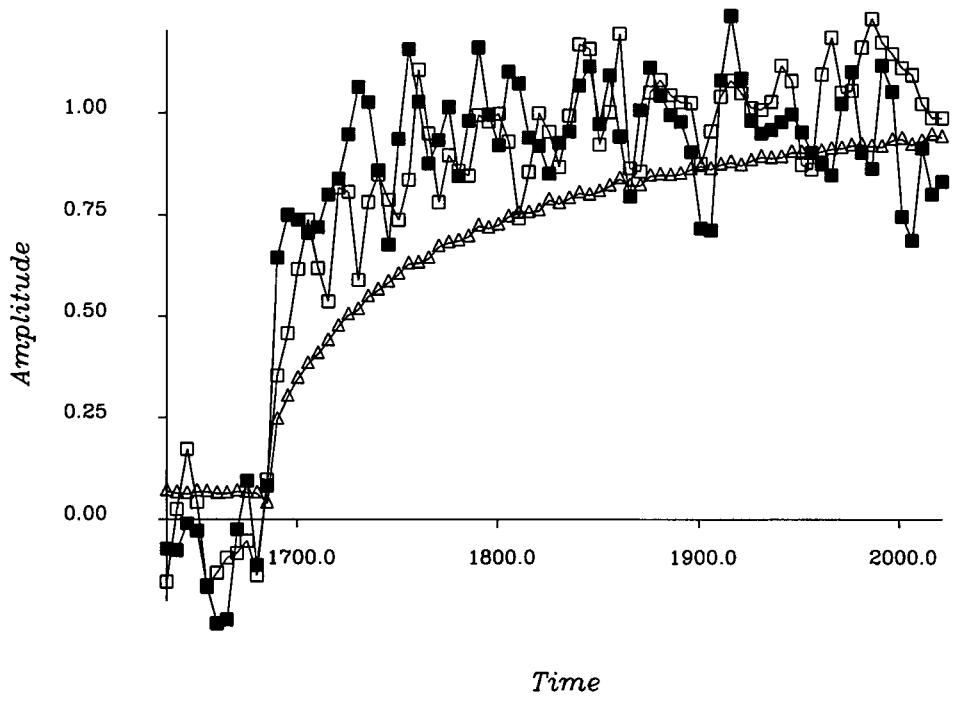

FIGURE 2 Changes in the equatorial 10 (■) and 11 (□) intensities with force (△) following photolytic release of calcium from NP-EGTA. Data have been averaged from nine bundles used during a single experimental run. Zero dextran; time resolution, 5 ms; fiber number Z82 (June, 1998). Time axis here and in Figs. 3–9 shows values in milliseconds.

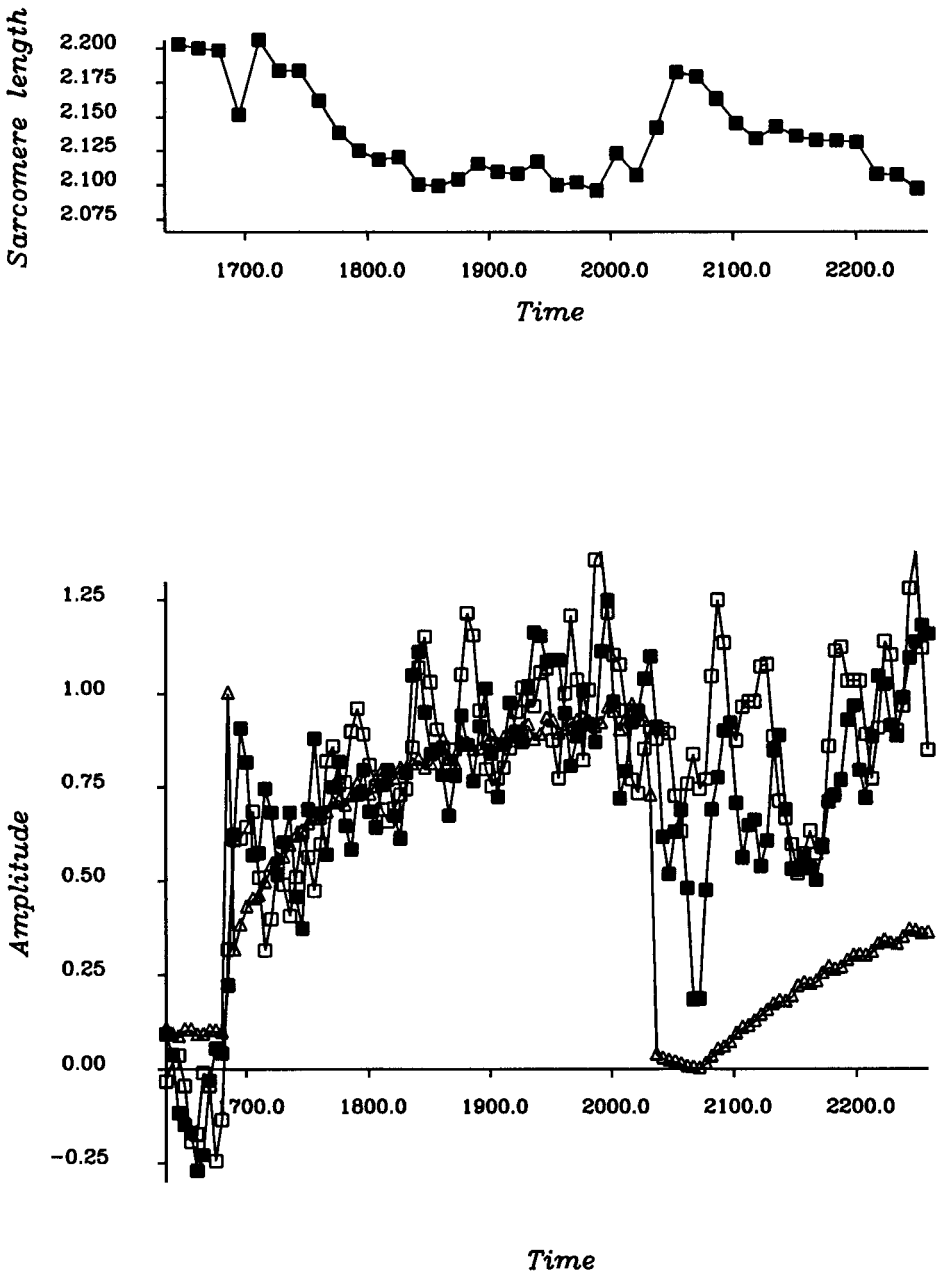

FIGURE 3 Changes in I_{10} (■) and I_{11} (□) and force (△) during activation and during shortening at $0.6V_{max}$ at the tension plateau. Time resolution, 5 ms; exposure time per point, 10 ms (i.e., product of sampling time and the number of summed responses); maximum tension, 247 kN m^{-2}; $t_{1/2}$ = 52 ms. Sarcomere length is invalid beyond the start of the release because the laser reflection passed off the face of the detector. Due to slight activation in the loading solution, force during shortening fell below the pre-flash level. It subsequently recovered to 27% P_o. Fiber number Z62 (June, 1998); zero dextran.

The compressed lattice

In Fig. 4, force and spectra have been averaged from five bundles from a single beam time. I_{10} decreased by 49 ± 2% (n = 7), subsequently decreasing a little further at a slower rate, whereas I_{11} increased by 94 ± 15% (n = 7). In experiments at a similar lattice spacing in single, intact muscle fibers from *Rana temporaria*, Griffiths et al. (1993a) found that isometric tetanic stimulation at full overlap caused a fall in I_{10} of 46.5% and a rise in I_{11} of 139.7%. Relative to background scattering, I_{11} was much weaker in skinned fibers than in intact cells, whereas I_{10} was virtually unaltered, which may result from an increased lattice disordering during skinning (Vainshtein, 1966; Hoskins et al., 1999), and the smaller change in I_{11} accompanying activation implies that this disorder increased as tension developed. I_{11}/I_{10} changed from 0.35 ± 0.03 (n = 7) in the relaxed state to 1.26 ± 0.06 (n = 7) at the isometric tension plateau. The value of I_{11}/I_{10} in the relaxed state was significantly smaller than in the uncompressed lattice ($p < 0.001$), but at the tension plateau the difference was not significant.

Table 1 contains a summary of the time courses of both intensity changes and the rise of force. In both the expanded and the compressed lattice, we found similar rates of change

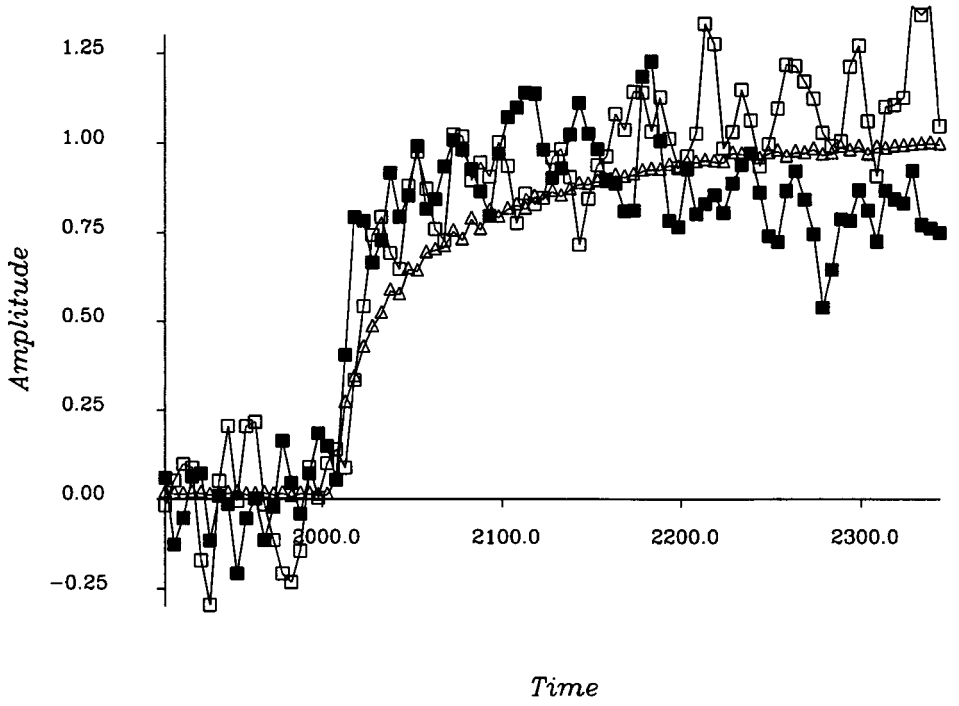

FIGURE 4 Changes in the equatorial 10 (■) and 11 (□) intensities with force (△) in the presence of 3% dextran. Data were averaged from five bundles. Time resolution, 5 ms; fiber number Y82 (May, 1997).

for each parameter. In the compressed lattice, the $t_{1/2}$ of the I_{10} fall was 24 ± 2 ms (n = 14), whereas the rise in I_{11} was again more rapid ($t_{1/2}$ = 15 ± 3 ms; n = 12).

Fig. 5 shows intensity changes from a single bundle that occurred during shortening in the presence of 3% dextran. The intensity changes at the release were very similar to those observed in zero dextran. I_{10} reached a value of 81.7 ± 6.2% of the change observed on activation, and I_{11} dropped to 69.9 ± 9.8% of its change at the tension plateau. Mean tension during shortening was 0.140 ± 0.115 P_o (mean ± SD). Changes in intensity were delayed with respect to force. Force recovery after shortening (0.815 ± 0.073 P_o (mean ± SD)) was associated with recovery to 110.2 ± 9.8% and 66.9 ± 21.2% of the initial activation

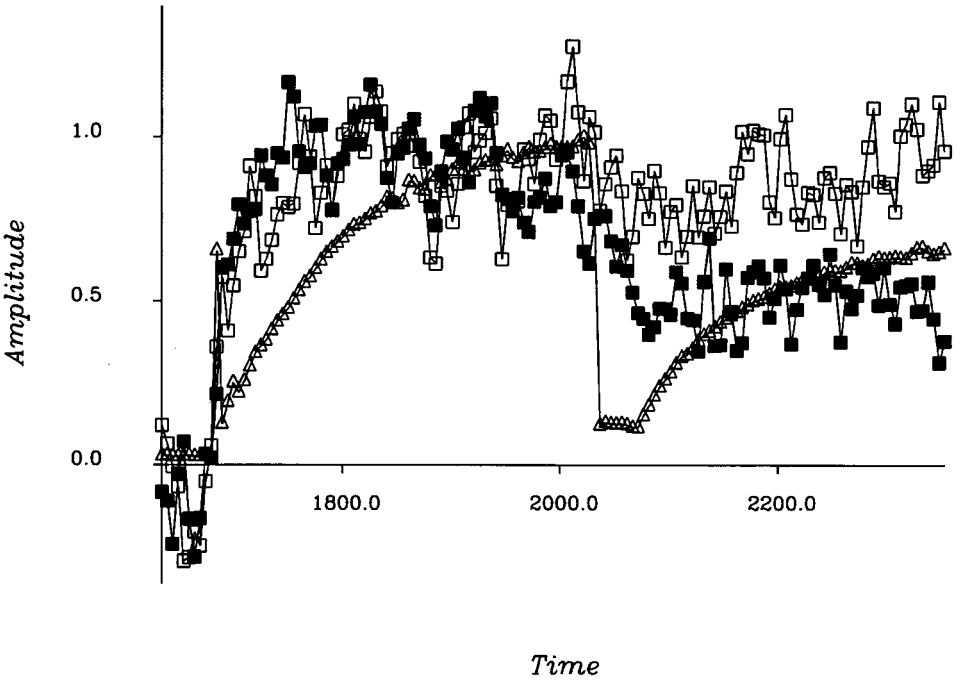

FIGURE 5 Changes in I_{10} (■) and I_{11} (□) and force (△) during activation and during shortening at $0.6V_{max}$ at the tension plateau in the presence of 3% dextran. Time resolution, 5ms; exposure time per point, 10ms; maximum force, 132 kN m^{-2}; $t_{1/2}$ = 25 ms. Force was discharged to 0.12 P_{max} during shortening and subsequently recovered almost to P_o. Fiber number Z12 (June, 1998).

changes in I_{10} and I_{11}, respectively, again suggesting a possible movement effect on the isotonic intensity levels. Unfortunately, during these experiments, it was not possible to maintain a laser diffraction pattern sufficiently long to record sarcomere length during the release, either through deterioration or passage of the reflection from the face of the detector.

Lattice spacing changes

The uncompressed lattice

Figs. 6 and 7 show changes in lattice spacing during activation in the absence of dextran. The rise of isometric tension was accompanied by a decrease in spacing. The mean compression was 1.5 ± 0.6% (n = 21) from a relaxed spacing of 46.7 ± 0.2 nm. Lattice compression was rapid ($t_{1/2}$ 18 ± 4 ms; n = 10) and preceded force by 22 ms (see Table 1). The spacing decrease consisted of an initial rapid decline followed by a slower compression phase (Fig. 6).

Shortening was accompanied by an increase in lattice spacing (Fig. 7). The mean expansion was 2.4 ± 0.3% (n = 12) to 47.4 ± 0.3 nm whereas tension was at a minimum. The spacing during release exceeded the spacing in the relaxed state (see Table 2). Taking the mean force during shortening ($0.141P_o$), this gave a force-compression ratio (i.e., the ratio of lattice compression to the change in axial load (Hoskins et al., 1999)) of 1.0×10^{-2} nm/(kN m^{-2}) in the calcium-activated state, half the value in the 2,3-butanedione 2-monoxime (BDM)-activated state of Hoskins et al. (1999).

The recoil of lattice spacing coincided with the onset of shortening and then remained constant while tension was low, indicative of an elastic response to the discharge of force, not to the shortening per se. The expansion was similar to that seen in intact fibers allowed to shorten at the tetanus plateau, where the spacing change during shortening also partially reversed the compression associated with activation (Bagni et al., 1994).

Tension recovery was accompanied by a small compression of the lattice toward its value to the tension plateau. The mean recompression was 1.1 ± 0.6%, (n = 12) but was found not to be statistically significant. The spacing recovery was much smaller than that observed in intact fibers (Bagni et al., 1994), particularly under hypotonic conditions, where the intact fiber lattice was expanded (close to the spacing of uncompressed fibers used here) and where spacing recovery after shortening was enhanced (Bagni et al., 1994).

The compressed lattice

Addition of 3% dextran T500 compressed the lattice in the relaxed state to a mean spacing of 42.6 ± 0.3 nm (n = 17) (see Table 2), close to the lattice spacing observed in intact frog skeletal muscle fibers (40–42 nm at 4°C (Bagni et al., 1994) at 2.2 μm).

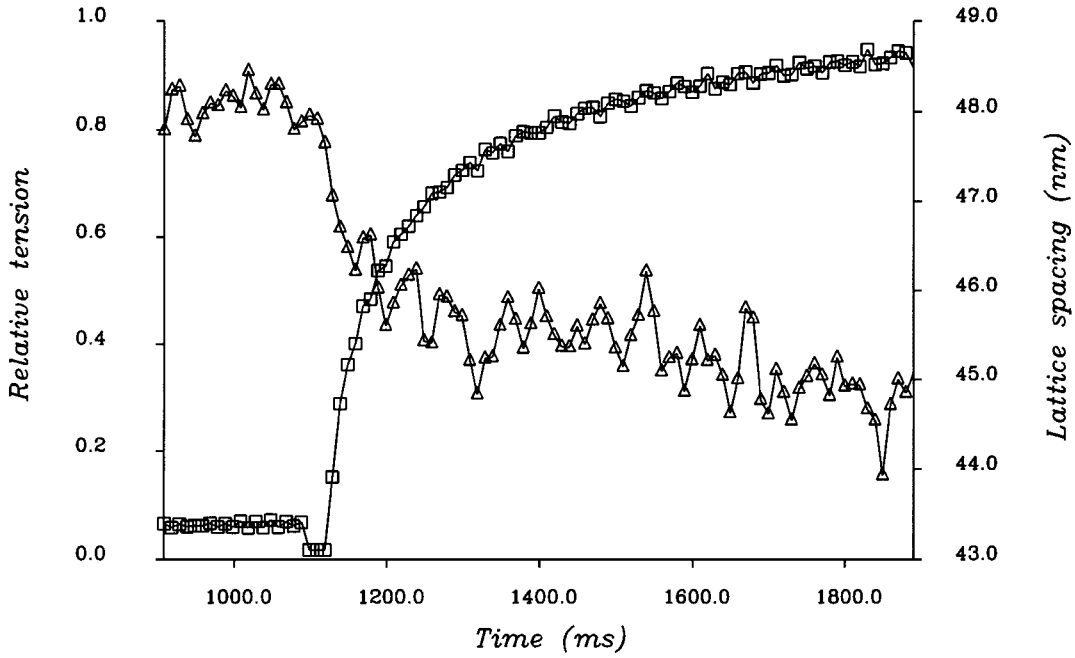

FIGURE 6 Lattice spacing (△) and tension (□) following activation by photolytic release of calcium from NP-EGTA. In this fiber, the relaxed lattice spacing was exceptionally large, which resulted in a particularly clear compression phase following the flash. Time resolution, 10 ms; exposure time per point, 30 ms. Force rose to 181 kN m^{-2} with $t_{1/2}$ = 50 ms. Zero dextran; fiber number Z27 (September, 1996).

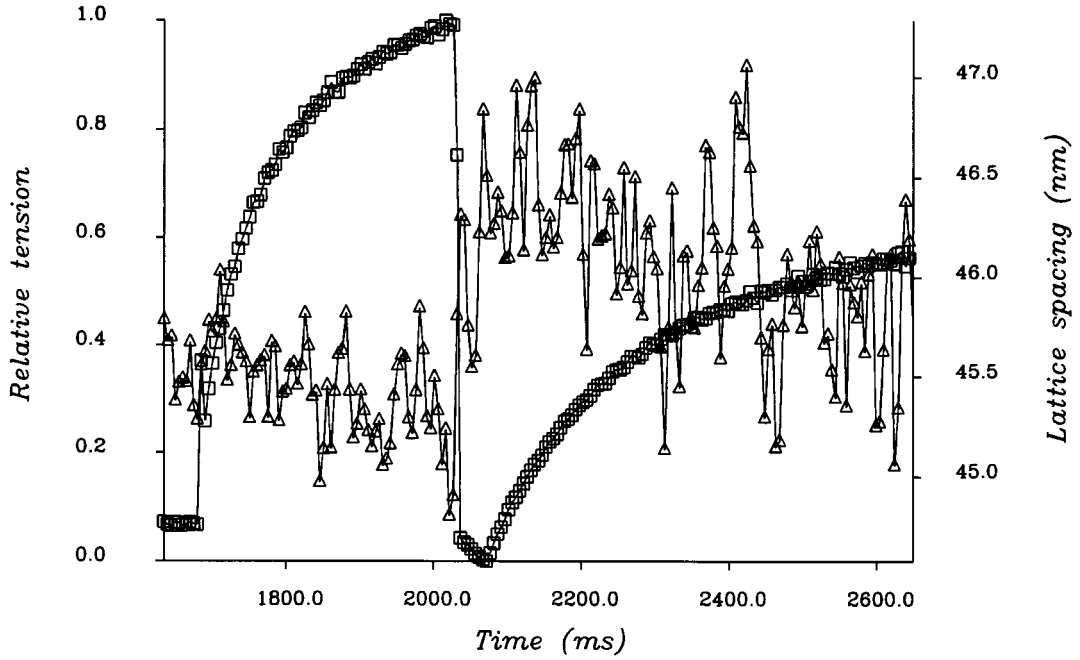

FIGURE 7 Lattice spacing (△) and force (□) during activation and ramp release at the tension plateau (fiber was allowed to shorten at $0.75V_{max}$). Time resolution, 5 ms; exposure time per point, 10 ms; maximum tension, 81 kN m^{-2}; $t_{1/2}$ = 52 ms. During the release tension was discharged to 5% P_o and during the recovery it returned to 42% P_o. Zero dextran; fiber number Z82 (June, 1998).

Figs. 8 and 9 show the lattice spacing changes that accompanied activation in the presence of 3% dextran. The compression observed during tension rise in the uncompressed lattice was replaced by a lattice expansion in the compressed fibers. The mean expansion between the relaxed state and the isometric tension plateau was 2.7 ± 0.7% (n = 17).

Lattice spacing increased rapidly following the flash (Fig. 8). An initial, rapid increase was followed by a slower phase during which spacing continued to increase. In some instances the slower phase was much reduced (see Fig. 9). The $t_{1/2}$ of the expansion (16 ± 3 ms; n = 7) was similar to that of the corresponding compression under zero dextran conditions (see Table 1).

Fig. 9 shows the response to a release at the isometric tension plateau in the presence of 3% dextran. In this preparation, we were able to obtain both lattice spacing and sarcomere length measurements during the rise of isometric tension, and four examples of the profile of the first-order diffracted laser beam are shown. It can be seen that as tension developed, lattice spacing increased rapidly. Discharge of tension caused a further spacing increase. In fibers allowed to shorten, mean spacing increased by 2.7 ± 0.4% from the tension plateau to 45.0 ± 0.4 nm during isotonic shortening. Tension recovery was accompanied by a small recompression of the muscle lattice, but the mean recompressed spacing was not statistically different from that during the release. Taking the mean force during shortening

TABLE 2 Mean lattice spacing at various stages of contraction induced by photolytic release of Ca^{2+} from NP-EGTA

State	Lattice spacing (uncompressed)	Lattice spacing (compressed by 3% dextran)
Relaxed (a1)	46.71 ± 0.25 nm (21)	42.63 ± 0.28 nm (17)
Tension plateau (a2)	46.02 ± 0.24 nm (21)	44.01 ± 0.29 nm (17)
Change on activation (a2-a1)	−0.68 ± 0.30 nm (21)	1.37 ± 0.28 nm (17)
During isotonic shortening (a3)	47.40 ± 0.31 nm (12)	45.04 ± 0.43 nm (10)
Change on shortening (a3-a2)	1.09 ± 0.45 nm (12)	1.20 ± 0.53 nm (10)
After tension recovery (a4)	47.20 ± 0.30 nm (12)	45.04 ± 0.42 nm (10)

Values are mean ± SE with the number of experiments in parentheses. Parameter (a2-a1) was significantly different between 0% and 3% dextran experiments at $p < 0.001$, whereas (a3-a2) was not significantly different at $p = 0.5$ between these conditions, nor was the spacing during recovery significantly different from that during release. The change in spacing after photolysis of caged calcium was significant in uncompressed fibers ($p < 0.1$) and highly significant in compressed fibers ($p < 0.005$). Spacing a3 was significantly different from a2 in both uncompressed fibers ($p < 0.025$) and compressed fibers ($p < 0.1$).

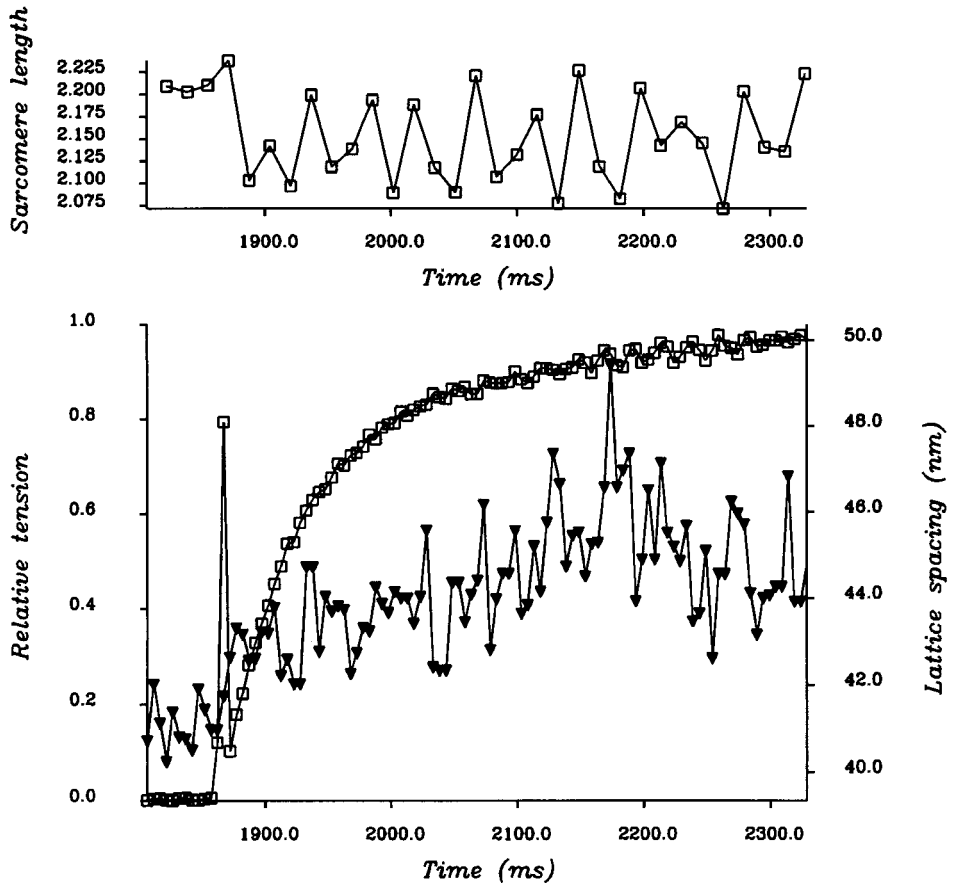

FIGURE 8 Lattice spacing (▼) and force (□) following photolysis of NP-EGTA in the presence of 3% dextran. Time resolution, 5 ms; exposure time per point, 5 ms. Laser intensity declined during activation in this fiber, causing indecision in the calculated sarcomere length beyond the first few points after the flash. The points lying close to 2.1 μm are the more representative of the true sarcomere length. Force rose to 140 kN m^{-2} with $t_{1/2}$ = 50 ms. Fiber number C56 (November, 1997).

as 0.14P_o, the corresponding expansion of the lattice would give a force-compression ratio (Hoskins et al., 1999) of 1.2 nm/(kN m^{-2}).

The finding that the spacing changes during tension rise were in opposite directions in the compressed and uncompressed lattice suggests the existence of an equilibrium spacing at which activation would result in neither an expansion nor a compression of the lattice, a situation described previously from static studies of spacing and activation (Maughan and Godt, 1980; Matsubara et al., 1984; Brenner and Yu, 1991). The change in lattice spacing observed upon activation is plotted as a function of the relaxed spacing in Fig. 10. It can be seen that the extent of the spacing change during activation was related to the initial spacing in the relaxed state. Assuming this relation to be a linear regression of spacing change upon initial spacing, we obtained a trend line that intercepted the abscissa at an equilibrium spacing of 45.35 nm (41.12–49.66 nm for 95% confidence interval). This finding contrasts strongly with the observation that discharge of axial tension during shortening always produced a lattice expansion, which suggests a compressive cross-bridge radial force component at all spacings in these experiments.

DISCUSSION

Tension and intensity changes during activation

Following NP-EGTA photolysis, tension rose to 119 kN m^{-2} ($t_{1/2}$ = 40 ms at 5°C), with or without dextran. P_o was similar to that obtained when activating with a Ca-EGTA solution of pCa 4.5 (121 ± 8 kN m^{-2}) and in agreement with a P_o of 148 ± 9 kN m^{-2} measured by Ferenczi et al. (1984) in frog skinned skeletal muscle fibers at 0–5°C. The $t_{1/2}$ of tension rise was similar to that measured in intact frog fibers and electrically stimulated whole muscle (38–45 ms between 4°C and 8°C (Kress et al., 1986; Cecchi et al., 1991; Bordas et al., 1993)). Activation by UV photolysis of NP-EGTA is therefore closely analogous to tetanic stimulation of intact fibers.

Flash UV intensity is diminished during passage through the fiber, both through absorption by the fiber and NP-EGTA, and by scattering of the beam from its original light path. Intensity loss may be estimated from variation in the ratio of logarithms of fiber fluorescence and radius at the appropriate exciting wavelength. Log I/log a = 2 (direct proportionality between fluorescence and fiber volume) in the absence of diminishment of the exciting or emitted

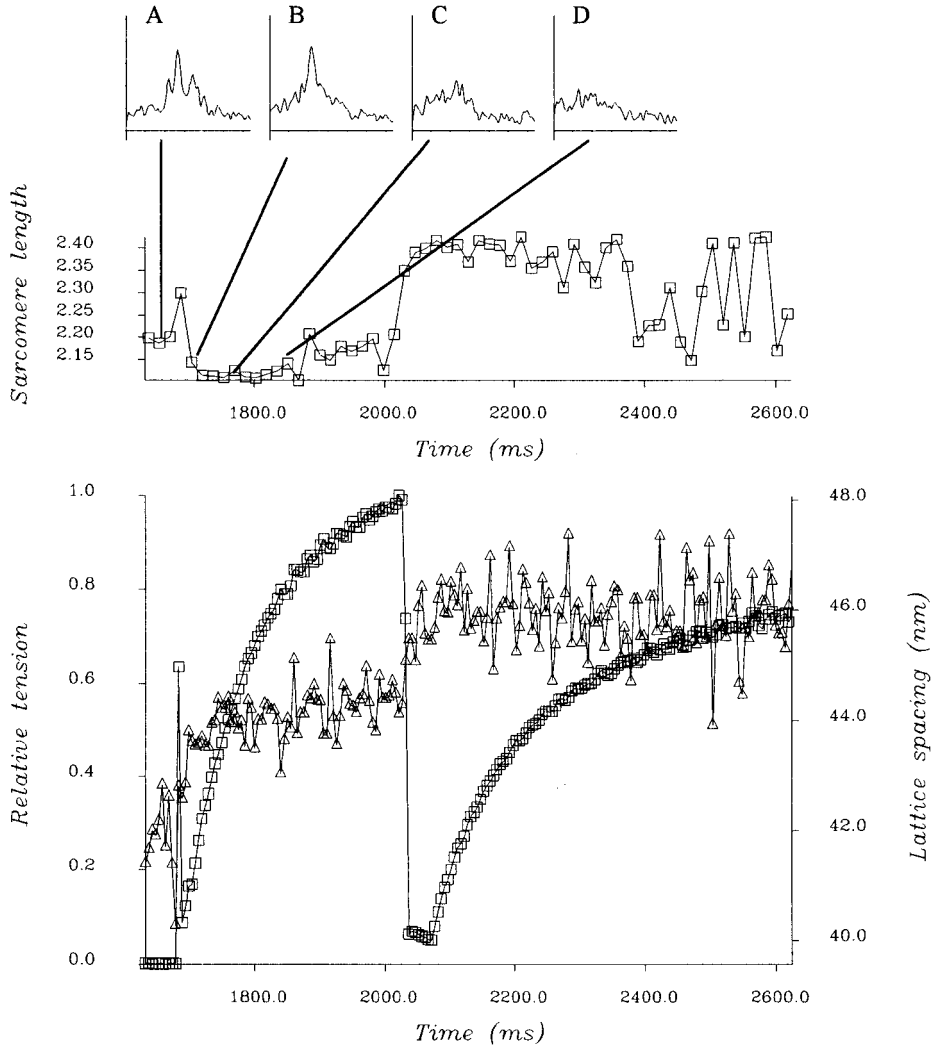

FIGURE 9 Lattice spacing (△) and force (□) during activation and ramp release in the presence of 3%dextran as above. Spectra A, B, C, and D are the scanning photodiode array output at the corresponding points on the sarcomere length plot (*upper panel*). The pronounced peak in the relaxed laser pattern disappeared rapidly following activation, and the reflection became less intense and shifted to the left. During the ramp release, the first-order laser reflection was lost from the face of the array, and the sarcomere length output from this point is not valid. Time resolution, 5 ms; exposure time per point, 10 ms; maximum tension, 185 kN m^{-2}; $t_{1/2}$ = 61 ms. At the release tension was discharged to 7% P_o; during recovery it returned to 79% P_o. Fiber number Z09 (June, 1998).

beam. Taking the worst case, that log I/log a arose solely through diminished excitation intensity, total fluorescence intensity would be given by

$$I_{total}(a) = 2\frac{I_o}{k}\int_0^a (1 - e^{-2k\sqrt{a^2-y^2}})dy, \qquad (1)$$

where I_o is incident intensity, and x and y are Cartesian coordinates defining a cylindrical fiber of radius a. Eq. 1 may be solved using an open-ended Romberg integration algorithm (Press et al., 1989) to obtain I_{total} as a function of a. Values for log I_{total}/log a have been found experimentally for both rabbit psoas skinned fibers loaded with 10 mM NADH (1.64; $\lambda_{excitation}$ = 340 nm, $\lambda_{emission}$ = 470 nm (Griffiths et al., 1980)) and for the autofluorescence of intact barnacle muscle (1.63; $\lambda_{excitation}$ = 325 nm, $\lambda_{emission}$ = 440 nm (Griffiths et al., 1988)). Assuming an absorption coefficient (k) of 14,506 m^{-1} (equal to 10^2 ln(10) [NADH] $\epsilon_{\lambda=340\,nm}$; $\epsilon_{\lambda=340\,nm}$ = 6.3 mM^{-1} cm^{-1}), log I_{total}/log a from Eq. 1 in the a range of Griffiths et al. (1980) was 1.52, close to the observed value, indicating that intrinsic fiber absorbance was small compared with NADH absorbance. Griffiths et al. (1988) obtained log I_{total}/log a by changing fiber length (a varied in the range 500–750 μm). Applying Eq. 1, their ratio corresponds to a k of 1100 m^{-1} for intrinsic fiber absorbance and scattering, which is almost entirely accounted for by indigenous NADH absorbance ([NADH] of ~0.8 mM). The molecular extinction coefficient ($\epsilon_{\lambda\,=\,347\,nm}$) of NP-EGTA is 0.974 mM^{-1} cm^{-1}, giving a k of 637 m^{-1} at 2.84 mM. Both these studies point to a much lower k for intrinsic absorbance of skinned fibers at 340 nm, so we would expect NP-EGTA to be the main source of absorbance for loaded bundles. In this study, bundles had diameters of 120–175 μm, so taking k as 637 m^{-1}, the fraction (1 − A(a)) of bundle cross-sectional area exposed to more than 90% of I_o would have been between 98% and 100%, given by

$$1 - A(a) = \frac{2\theta}{\pi} - \frac{l}{\pi a^2}\sqrt{a^2 - \frac{l^2}{4}}, \qquad (2)$$

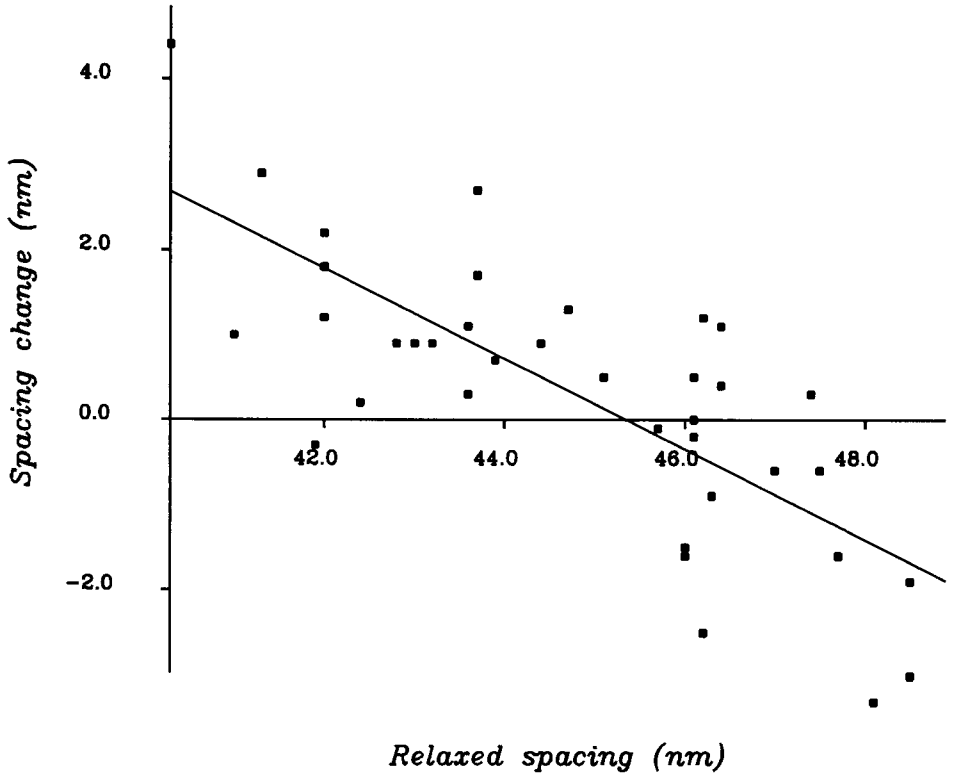

FIGURE 10 Variation in spacing change during activation with lattice spacing in the relaxed state. The data were best fit by the straight line $y = -0.532x + 24.145$ ($r = 0.77$; $p < 0.001$), giving an x-axis intercept of 45.35 nm.

where l is the path length in the fiber for 90% transmission, and θ is the angle formed at the intersection between a transmitted beam of path length l and the radius vector of the bundle. A 10% fall in intensity produces a variation in [NP-EGTA] photolyzed of 10% or less, depending on the photolysis rate at I_o. The mean concentration of NP-EGTA photolyzed is given by

$$\Delta[\bar{L}] = \frac{([\mathrm{Ca}]_t + K[\mathrm{Ca}^{2+}]_c[\mathrm{Ca}^{2+}]_r)([\mathrm{Ca}^{2+}]_c - [\mathrm{Ca}^{2+}]_r) + [\mathrm{Ca}^{2+}]_r[\mathrm{CaTn}](1 + K[\mathrm{Ca}^{2+}]_c)}{K[\mathrm{Ca}^{2+}]_c[\mathrm{Ca}^{2+}]_r}, \quad (3)$$

where subscripts c and r refer to activated and relaxed $[Ca^{2+}]$, respectively, $[Ca]_t$ is the total calcium in the loading solution, [CaTn] is the total troponin-bound calcium concentration, and K is calcium affinity of NP-EGTA (1.25×10^7 M^{-1}). $[Ca^{2+}]_r$ is calculated from $[Ca]_t$, [NP-EGTA], and K. $[Ca^{2+}]_c$ may be obtained by assuming 95% activation, reached at pCa 5.8 (Godt and Lindley, 1982). Mean photolysis is related to absorbance over a light path by

$$\Delta[L(x)] = \frac{\pi a^2 \Delta[\bar{L}]}{I_{\mathrm{total}}(a)} e^{-\mathrm{kx}}. \quad (4)$$

We may now estimate $[Ca]_c$ from Eqs. 3 and 4 at the 90% I_o boundary for the largest fiber bundles (radius = 88 μm) as 0.71 μM (pCa 6.146), which would correspond to 63% activation (Godt and Lindley, 1982). We therefore conclude that our preparations would have been activated throughout their cross section by the flash, and this activation would varied locally by less than 37%, even in the largest bundles used.

The $t_{1/2}$ of I_{10} and I_{11} signals accompanying activation of frog muscle intact fibers is 25–30 ms, whereas the $t_{1/2}$ for the rise of tetanic tension is 40–50 ms, giving a lead of the equatorial signals over force of ~20 ms (Kress et al., 1986; Cecchi et al., 1991; Bordas et al., 1993; Griffiths et al., 1993b). In electrically stimulated fish muscle, however, the rise in I_{11} led the fall in I_{10}, and the I_{10} time course closely resembled that of tension (Harford and Squire, 1992). There has been no previous detailed presentation of corresponding x-ray diffraction data from muscle activated by caged calcium photolysis. A report by Brenner et al. (1989) showed a lead of I_{11} over isometric tension development of 70 ms, using photolysis of [1-(2-nitro-4,5-dimethoxyphenyl)-1,2-diaminoethane-N,N,N′,N′-tetraacetic acid] (DM nitrophen) to Ca-activated frog skinned fibers, but tension development was very slow ($t_{1/2}$ = 100 ms at 7°C) compared with tetanized fibers. Poole et al. (1989) obtained force activation rates more similar to those reported here, using DM nitrophen photolysis to activate rabbit skinned psoas muscle, and found a 30–40-ms lead of equatorial intensities over force, without separation of I_{10} and I_{11}. Because DM nitrophen has a relatively high magnesium affinity, these findings are complicated by simultaneous, photolysis-induced changes

in both [Ca^{2+}] and [Mg^{2+}]. This is not the case with NP-EGTA, whose magnesium affinity is much lower and does not change appreciably on photolysis. Our experiments show a 13–25-ms lead of equatorial signals over force, with I_{11} leading I_{10} by ~8 ms, although this lead was of low statistical significance for uncompressed fibers ($p < 0.2$). This lead may arise from formation of low-force bridges before force generation (Kress et al., 1986; Bordas et al., 1993; Harford and Squire, 1992; Griffiths et al., 1993a), and subsequent changes in I_{10} and force may be related to redistribution of bound cross-bridges to favor a force-generating configuration (Harford and Squire, 1992). Theoretically, during a power stroke based on S1 rotation, an I_{10} signal could occur with only small changes in I_{11} (Malinchik and Yu, 1995). A lead of I_{11} over I_{10} was observed in intact fiber studies of activation in frog (Cecchi et al., 1991), but was not deemed significant.

Displacement of the fiber from its optimum position in the beam during activation could accelerate I_{11} changes and retard I_{10}, but would both reduce the activation-induced change in I_{11} and increase the change in I_{10}. Because the change in I_{10} and I_{11} on activation was close to that observed in intact fibers, we feel this effect is unlikely to account for the lead of I_{11}. As sarcomere length showed relatively small changes during tension generation and as during shortening we find that I_{11} reduction was greater than I_{10} elevation, any effect on $t_{1/2}$ from the transient establishment of an isotonic-like equatorial pattern should have been small and should have retarded the I_{11} signal more than I_{10} and, therefore, would not explain the lead of I_{11}. The resting sarcomere length of 2.2 μm was in the region of full overlap between the thin and thick filaments, where equatorial intensities and force generation are relatively insensitive to sarcomere length changes. If the sarcomere length increased beyond 2.2 μm, the principal effect is a reduction of I_{11} (Griffiths et al., 1993a), which should induce similar effects to those discussed above for movement artifacts, and which we reject for the same reasons. Therefore, any effects on the relative I_{11} and I_{10} kinetics due to changes in position in the beam, myofilament overlap, or shortening are probably negligible. It is more likely that, because flash photolysis activation is more rapid and uniform, it revealed a lag between I_{11} and I_{10} signals that was obscured by the more complex process of intact cell activation. This is supported by the faster $t_{1/2}$ for both equatorial signals reported here, compared with intact fibers (cf. Table 1 with intact cell $t_{1/2}$ of 33.2 ms (I_{10}) and 27.6 ms (I_{11}) (Cecchi et al., 1991)).

Both the relaxed I_{11} and the I_{11} change on activation in the presence of dextran were smaller than observed in tetanized intact single fibers (Griffiths et al., 1993a), whereas I_{10} and lattice spacing were similar. Radial disorder of the A-band can cause a more marked reduction in I_{11} than I_{10} and may be the cause of this effect, especially as disorder effects were seen with prolonged skinning (Hoskins et al., 1999). Preliminary experiments showed a sensitivity of I_{10} and I_{11} to anions used in skinned fiber solutions, so a direct effect of ionic environment cannot be excluded.

Lattice spacing changes during activation

Activation was accompanied by a lattice compression of 1.5 ± 0.6% ($n = 21$) in zero dextran, or an expansion of 3.2 ± 0.7% ($n = 17$) in 3% dextran. Intact fiber activation was accompanied by a brief initial lattice expansion (Bagni et al., 1994), which was attributed to constant volume effects of a small amount of fiber shortening. Under hypotonic conditions, the rise of tetanic tension was accompanied by lattice compression without this initial expansion phase (Bagni et al., 1994). Our spacing changes for the compressed lattice were too large to be accounted for by changes in sarcomere length (3% during tension development compared with 2–3% for intact cells (Huxley, 1979) with whole muscle (Cecchi et al., 1991) in intact single fibers) and therefore indicate development of an expansive force during activation. This suggests that the initial lattice expansion of intact cells at standard tonicity may also arise, in part, from an expansive force developed on activation rather than entirely from internal shortening. The 1.5% fall in lattice spacing in the uncompressed lattice could be explained by a 3.1% increase in sarcomere length in a constant-volume system, but most sarcomere records exhibited shortening in zero dextran. Hoskins et al. (1999) found constant-volume-like behavior in skinned fibers, but only in the relaxed state, and then only in the dynamic response to very rapid length steps. Spacing of cross-bridge-bound states correlated more closely with the change in force, suggesting that constant-volume constraints in the relaxed fiber were overcome by a cross-bridge-generated radial force, either by expulsion of fluid from the sarcomere or by a rapid redistribution of sarcoplasm between the I and A bands.

The spacing change upon activation could be approximated to a linear regression upon the relaxed spacing. There was a good match between the data with and without dextran (Fig. 10). However, the equilibrium spacing thus determined (45.35 nm) differs greatly from that found from static experiments by Brenner and Yu (1991) of 39 nm in rabbit psoas fibers, or by Bagni et al. (1994) for intact fibers from frog tibialis anterior, where a small compression was still observed during recovery of axial tension at a spacing of 38 nm. The species difference between Brenner and Yu (1991) and our experiments seems unlikely to explain the difference in equilibrium spacing, because the rigor equilibrium spacing in rabbit (44 nm) is somewhat larger than the value shown in Matsubara et al. (1984) for frog. If the activated equilibrium spacing were shifted in the same manner, a value smaller than 39 nm would have been expected. Our equilibrium spacing is not greatly different from that of Irving et al. (1998) of 44 nm, determined from tetanic activation of frog sartorius muscle at different tonic-

ities, a method similar to the photolysis activation technique used here. On the other hand, the effect on spacing of axial force discharge by a release was an expansion in all cases in the present work, which implies the discharge of a compressive cross-bridge radial force, and which is more consistent with an equilibrium spacing close to that of Brenner and Yu (1991). Radial forces acting on the lattice have been recently reviewed by Millman (1998). He points out that larger estimates of equilibrium spacing may arise from the presence of rigor bridges (which have a larger equilibrium spacing) in experiments performed without an ATP backup system. But this cannot explain the findings of Irving et al. (1998) from live muscle, or the present findings, where a backup system was present and where discharge of cross-bridge force indicated a smaller equilibrium spacing than that found by activation. It therefore seems likely that this disparity of equilibrium spacings arises from the difference between spacing changes measured during discharge of isometric tension (Bagni et al., 1994) or static activation (Brenner and Yu, 1991) and spacing measured dynamically during the activation process (Irving et al., 1998; present observations). This could arise from the development of a transient expansive force during activation, whose origin is presently unknown.

In the uncompressed lattice, the initial phase of compression was rapid and preceded force by approximately 25 ms, being complete by the time force had reached ~60%. This may relate to the work of Brenner and Yu (1985) who found a larger change in lattice spacing with isometric force below $0.5P_o$. As can be seen in Table 1, the $t_{1/2}$ of lattice expansion in the presence of dextran, of compression in zero dextran fibers, and of I_{11} increase accompanying activation were very similar, suggesting that the same structural change may underlie all three phenomena.

Intensity during shortening at low load

The reported behavior of the 1,0 and 1,1 reflections during shortening is surprisingly variable. Yagi et al. (1993b) found a fall in both I_{10} and I_{11} during shortening, but after correction for sarcomere length changes reported a rise in I_{10} and a fall in I_{11}. Yagi et al. (1993a), using image plates, found a fall in intensity of both reflections. Yagi and Takemori (1995) measured a 16% decrease in I_{11}, whereas I_{10} remained constant in intact frog sartorius muscle shortening at loads of less than $0.3P_o$. Others (Huxley, 1979; Huxley et al., 1988; Griffiths et al., 1991, 1993a,b) found a larger decrease in I_{11} and a similar relative increase in I_{10} during shortening at less than $0.1P_o$ or insignificant change in either intensity during shortening (Podolsky et al., 1976). It is possible that changes in excitation occur as a result of shortening, causing the effects on I_{10} and I_{11} to become obscured in intact fibers. No comparable experiments on skinned fibers, where sarcoplasmic $[Ca^{2+}]$ can be more precisely controlled, had previously been performed because of the difficulty of preserving structural order during the required prolonged activation. Our new findings avoid these limitations by using flash photolysis, permitting us to obtain data during isotonic shortening within 400 ms of activation while retaining the advantages of the skinned fiber preparation. We find significant changes in I_{10} and I_{11}, but a relatively smaller change in I_{10} (29% of activation intensity fall, compared with 45.5% of activation intensity rise for I_{11} in the uncompressed lattice). The I_{10} signal would be reduced, and the I_{11} signal enhanced, from a fiber displaced from the optimal position in the beam during shortening, so the smaller I_{10} signal reported here may not represent a departure from the behavior of the intact fiber, where the fractional intensity changes were similar for I_{10} and I_{11}, i.e., ~45% reversal of the change produced on activation during shortening at less than $0.1P_o$ (Huxley, 1979; Huxley et al., 1988; Griffiths et al., 1991, 1993a,b). Griffiths et al. (1993a) showed that during shortening at $0.14P_o$, equatorial signals from intact fibers changed by ~25% of the intensity change during activation, with the I_{10} fractional change being slightly larger than I_{11}. In the compressed lattice, I_{10} was reversed by 18.3% and I_{11} by 30.1%, in closer agreement with the values from the living cell preparation.

The relatively large intensity changes we report are inconsistent with the small intensity changes detected by others (Yagi et al., 1993a,b; Yagi and Takemori, 1995; Podolsky et al., 1976). During high-velocity shortening, very few myosin heads diffract with actin-based periodicities (Martin-Fernandez et al., 1994; Yagi and Takemori, 1995), suggesting a low fractional attachment of cross-bridges, in agreement with stiffness measurements and in conflict with the much smaller changes in equatorial signals. There is no theoretical requirement for I_{10} and I_{11} to be linear measures of attachment during shortening, but because they are almost linear indicators of isometric activation (Yu et al., 1979; Brenner and Yu, 1985), it is not unreasonable to assume that they might also be linear indicators of cross-bridge propinquity to actin in the isotonic condition. The apparent disparity between isotonic I_{10} and I_{11} changes and attachment measured by other means must then arise from S1 being located close to the thin filament but without generating stiffness or diffracting with actin periodicities. In other words, detached, but differing from their true relaxed-state configuration.

Lattice spacing changes during shortening

Lattice spacing increased during shortening irrespective of whether the activation spacing change was an expansion or a compression. This spacing increase was rapid and did not continue throughout the shortening period. In the presence of dextran, this shortening expansion further increased the spacing away from its relaxed value, which supports the evidence from intensity changes that shortening was not

accompanied by a restoration of the relaxed state for detached bridges. Instead, in the presence of dextran, a significant expansive radial force was acting during the release even when axial force was approaching zero, and in both the compressed and uncompressed lattice, a compressive force accompanied axial tension generation irrespective of whether activation resulted in a lattice expansion or a compression.

Brenner et al. (1996) found a larger equilibrium spacing for weakly binding bridges. If a large weakly binding state population accumulated during shortening, this could cause lattice expansion. However, spacing changes occurred much more rapidly than the accompanying intensity changes, which indicate changes in occupancy of cross-bridge states. Alternatively, because fibers shortened by up to 6.7%, this could lead to a lattice expansion by up to 3.3%, assuming constant volume, sufficient to account for the 2.4–2.7% expansion seen in our experiments. But spacing changes occurred promptly on discharge of isometric tension and did not progressively increase during the length ramp, suggesting that they were directly related to the change in load, and not the change in sarcomere length. Spacing changes during shortening in these experiments were approximately half the size of those found in intact fibers (Bagni et al., 1994). This suggests that spacing changes during shortening of intact fibers do contain a substantial constant-volume component that is absent or much reduced in the skinned fiber preparation. If spacing changes arose chiefly from discharge of radial cross-bridge forces during shortening, we may compare them with those obtained for other cross-bridge states by Hoskins et al. (1999). Although Hoskins et al. (1999) worked at much higher time resolution and applied smaller, step-form length changes, they concluded that, in both the rigor state and in calcium activation plus BDM, spacing changes were related to the change in load rather than the change in sarcomere length. They quantified this relation as the force-compression ratio, relating changes in spacing and axial load. The initial spacing changes after a length step in activated fibers plus BDM gave a force-compression ratio of 2×10^{-2} nm/(kN m^{-2}).in the absence of dextran. The corresponding value determined in this work for the calcium-activated fiber is smaller (1×10^{-2} to 1.2×10^{-2} nm/(kN m^{-2})) and very different from their rigor value (6.4×10^{-3} nm/(kN m^{-2})). In terms of the force-compression ratio, the rigor lattice is ~1.7-fold stiffer than the calcium-activated lattice, either because of a larger proportion of attached cross-bridges or a rigidity of the cross-bridge structure, which determines radial compliance. Static radial stiffness is roughly fourfold higher in rigor than in the calcium-activated state (Xu et al., 1993), whereas the ratio of cross-bridge stiffness between full activation and rigor is ~43% or smaller (Linari et al., 1998). It is clear that our dynamic force-compression ratio data lie closer to the axial stiffness data than to the static radial stiffness.

A notable difference from intact cell preparations is the recompression of the lattice after termination of active shortening. This was used by Bagni et al. (1994) as an index of radial force because it occurred in the absence of sarcomere length changes. The size of recompression depended on the tonicity of the bathing medium, being enhanced at low tonicity. Surprisingly, in the experiments reported here, recompression during force recovery was not a significant feature of lattice spacing changes. Recompression in dextran was smaller than in the uncompressed lattice, in accordance with the findings in intact fibers. If radial and axial forces are intimately connected, then this reduced recompression may be related to the incomplete recovery of tension after shortening in the skinned fiber preparation and the higher isotonic force to which tension was discharged. As activation and shortening occurred in air, both substrate supply and product removal from ATP hydrolysis were restricted. Taking an ATPase activity of 0.42 μM g^{-1} s^{-1} in tetanized, isometric frog muscle (Curtin et al., 1974), a partial specific volume of muscle proteins of 0.74 L kg^{-1}, and the density of muscle cells to be 1.06 kg L^{-1} (Ford et al., 1974), we may deduce 83% to be an estimate of the aqueous volume of a muscle cell, giving a phosphate production rate of 0.51 mM s^{-1}, close to the observed osmolyte production rate of 0.9 mOsmol L^{-1} s^{-1} (Rapp et al., 1998). So, during the course of a 1-s activation by caged calcium photolysis, 0.5–0.9 mM phosphate could accumulate in the fiber (taking the ATPase activity during high-velocity shortening as being close to isometric levels), which would be insufficient to reduce axial tension significantly, and this amount of ATP hydrolysis would be easily replaced without significant depletion of creatine phosphate stores. Therefore, we feel that the depression of force after shortening is not a consequence of the flash photolysis protocol or metabolite accumulation.

Overall, we find that flash activation of skinned muscle fibers produces equatorial intensity changes during activation and shortening resembling those observed in intact muscle fibers. This preparation therefore provides a good simulation of the tetanic response of living cells while providing a means by which procedures thought to modify activation or cross-bridge cycling may be studied in isolation from possible effects on membrane excitability or sarcoplasmic calcium, which could complicate intact cell studies. However, lattice spacing changes differed from those observed in intact cells, suggesting that although compressive cross-bridge forces act in both compressed and uncompressed fibers, an additional expansive force appears to be acting at the in vivo lattice spacing.

We express our thanks to the EMBL Outstation for experimental facilities, to Mr. B. H. Kunst for technical assistance, and to the Wellcome Trust and EU Large Installation Programme (CHGE-CT93–0040) for financial support.

REFERENCES

Ashley, C. C. M. A. Bagni, G. Cecchi, P. J. Griffiths, and G. Rapp. 1999. Submillisecond changes in myosin lattice spacing resulting from rapid length changes. *J. Mol. Biol.* 285:431–440.

Bagni, M. A., G. Cecchi, P. J. Griffiths, Y. Maeda, G. Rapp, and C. C. Ashley. 1994. Lattice spacing changes accompanying isometric tension generation in intact single muscle fibers. *Biophys. J.* 67:1965–1975.

Bordas, J., G. P. Diakun, F. G. Diaz, J. E. Harries, R. A. Lewis, J. Lowy, G. R. Mant, M. L. Martin-Fernandez, and E. Towns-Andrews. 1993. Two-dimensional time-resolved x-ray diffraction studies of live isometrically contracting frog sartorius muscle. *J. Muscle Res. Cell Motil.* 14:311–324.

Brenner, B., M. A. Ferenczi, M. Irving, J. Kaplan, R. M. Simmons, and E. Towns-Andrews. 1989. Structural changes upon activation of single isolated muscle fibers of the frog by photolysis of 'caged-calcium' studied by time-resolved x-ray diffraction. *J. Physiol.* 418:59.P.

Brenner, B., S. Xu, J. M. Chalovich, and L. C. Yu. 1996. Radial equilibrium lengths of actomyosin cross-bridges in muscle. *Biophys. J.* 71: 2751–2758.

Brenner, B., and L. C. Yu. 1985. Equatorial x-ray diffraction from single skinned rabbit psoas fibers at various degrees of activation. *Biophys. J.* 48:829–834.

Brenner, B., and L. C. Yu. 1991. Characterisation of radial force and radial stiffness in calcium activated skinned fibers of the rabbit psoas muscle. *J. Physiol.* 441:703–718.

Brust-Mascher, I., L. E. W. LaConte, J. Baker, and D. D. Thomas. 1999. Myosin light-chain domain rotates upon muscle activation but not ATP hydrolysis. *Biochemistry.* 38:12607–12613.

Cecchi, G., M. A. Bagni, P. J. Griffiths, C. C. Ashley, and Y. Maéda. 1990. Detection of radial cross-bridge force by lattice spacing changes in intact single muscle fibers. *Science.* 250:1409–1411.

Cecchi, G., P. J. Griffiths, M. A. Bagni, C. C. Ashley, and Y. Maéda. 1991. Time-resolved equatorial x-ray diffraction and stiffness during rise of tetanic tension in intact length-clamped single muscle fibers. *Biophys. J.* 59:1273–1283.

Corrie, J. E. T., B. D. Brandmeier, R. E. Ferguson, D. R. Trentham, J. Kendrick-Jones, S. C. Hopkins, U. A. van der Heide, Y. E. Goldman, C. Sabido-David, R. E. Dalee, S. Criddle, and M. Irving. 1999. Dynamic measurement of myosin light-chain-domain tilt and twist in muscle contraction. *Nature.* 400:425–430.

Curtin, N. A., C. Gilbert, K. M. Kretzschmar, and D. R. Wilkie. 1974. The effect of the performance of work on total energy output and metabolism during muscular contraction. *J. Physiol.* 238:455–472.

Elliott, G. E., J. Lowy, and C. R. Worthington. 1963. X-ray and light diffraction of the filament lattice in the living state and rigor. *J. Mol. Biol.* 6:295.

Ellis-Davies, G. C., and J. H. Kaplan. 1994. Nitrophenyl-EGTA, a photolabile chelator that selectively binds Ca^{2+} with high affinity and releases it rapidly upon photolysis. *Proc. Natl. Acad. Sci. U.S.A.* 91:187–191.

Ferenczi, M. A., Y. E. Goldman, and R. M. Simmons. 1984. The dependence of force and shortening velocity on substrate concentration in skinned muscle fibers from *Rana temporaria*. *J. Physiol.* 350:519–543.

Ford, L. E., A. F. Huxley, and R. M. Simmons. 1974. Tension responses to sudden length change in stimulated frog muscle fibers near slack length. *J. Physiol.* 269:441–515.

Godt, R. E., and B. D. Lindley. 1982. Influence of temperature upon contractile activation and isometric force production in mechanically skinned muscle fibers of the frog. *J. Gen. Physiol.* 80:279–297.

Godt, R. E., and D. W. Maughan. 1981. Influence of osmotic compression on calcium activation and tension in skinned muscle fibers of the rabbit. *Pflügers Arch.* 391:334–337.

Griffiths, P. J., C. C. Ashley, M. A. Bagni, Y. Maeda, and G. Cecchi. 1993a. Cross-bridge attachment and stiffness during isotonic shortening of intact single muscle fibers. *Biophys. J.* 64:1150–1160.

Griffiths, P. J., C. C. Ashley, M. A. Bagni, Y. Maeda, and G. Cecchi. 1993b. Time-resolved equatorial x-ray diffraction measurements in single intact muscle fibers. *Adv. Exp. Med. Biol.* 332:409–420.

Griffiths, P. J., C. C. Ashley, G. Cecchi, Y. Maéda, and M. A. Bagni. 1991. Equatorial x-ray diffraction pattern intensity during isotonic shortening or lengthening in single intact muscle fibers of *Rana temporaria*. *J. Physiol.* 438:146.P.

Griffiths, P. J., K. Güth, H. J. Kuhn, and J. C. Rüegg. 1980. ATPase activity in rapidly activated skinned muscle fibers. *Pflügers Archiv.* 387:167–173.

Griffiths, P. J., and A. Jones. 1994. A simple device for transfer of single muscle fibers by rotation between 70 μl chambers while making optical measurements. *J. Physiol.* 480:5.P

Griffiths, P. J., J. D. Potter, Y. Maéda, and C. C. Ashley. 1988. Transient kinetics and time-resolved x-ray diffraction studies in isolated single muscle fibers. *Adv. Exp. Med. Biol.* 226:113–128.

Harford, J. J., and J. M. Squire. 1992. Evidence for structurally different attached states of myosin cross-bridges on actin during contraction of fish muscle. *Biophys. J.* 63:387–396.

Hendrix, J., H. Fuerst, and D. Dainton. 201. 1982. A wire per wire detector system for high counting rate x-ray experiments. *Nucl. Instrum. Methods.* 201:139–144.

Highsmith, S. 1999. Lever arm model of force generation by actin-myosin-ATP. *Biochemistry.* 38:9791–9797.

Hoskins, B. K., C. C. Ashley, R. Pelc, G. Rapp, and P. J. Griffiths. 1999. Time-resolved equatorial x-ray diffraction studies of skinned muscle fibers during stretch and release. *J. Mol. Biol.* 290:77–97.

Huxley, H. E. 1969. The mechanism of muscle contraction. *Science.* 164:1356–1366.

Huxley, H. E. 1979. Time-resolved x-ray diffraction studies on muscle. *In* Cross-Bridge Mechanism in Muscle Contraction. H. Sugi and G. H. Pollack, editors. University of Tokyo Press, Tokyo. 391–401.

Huxley, H. E., and M. Kress. 1985. Crossbridge behaviour during muscle contraction. *J. Muscle Res. Cell Motil.* 6:153–161.

Huxley, H. E., M. Kress, A. R. Faruqi, and R. M. Simmons. 1988. X-ray diffraction studies on muscle during rapid shortening and their implications concerning crossbridge behaviour. *Adv. Exp. Med. Biol.* 226: 347–352.

Huxley, H. E., R. M. Simmons, A. R. Faruqi, M. Kress, J. Bordas, and M. H. Koch. 1981. Millisecond time-resolved changes in x-ray reflections from contracting muscle during rapid mechanical transients, recorded using synchrotron radiation. *Proc. Natl. Acad. Sci. U.S.A.* 78: 2297–2301.

Irving, T. C., Q. Li, B. Williams, and B. Millman. 1998. Z/I and A band lattice spacings in frog skeletal muscle: effects of contraction and osmolarity. *J. Muscle Res. Cell Motil.* 19:811–823.

Koch, M., and P. Bendall. 1981. *Proc. Digital Equip. Comput. Users Soc. (UK)* 13–16.

Kress, M., H. E. Huxley, A. R. Faruqi, and J. Hendrix. 1986. Structural changes during activation of frog muscle studied by time-resolved x-ray diffraction. *J. Mol. Biol.* 188:325–242.

Linari, M., I. Dobbie, M. Reconditi, N. Koubassova, M. Irving, G. Piazzesi, and V. Lombardi. 1998. The stiffness of skeletal muscle in isometric contraction and rigor: the fraction of myosin heads bound to actin. *Biophys. J.* 74:2459–2473.

Malinchik, S., and L. C. Yu. 1995. Analysis of equatorial x-ray diffraction patterns from muscle fibers: factors that affect the intensities. *Biophys. J.* 68:2023–2031.

Martin-Fernandez, M. L., J. Bordas, G. Diakun, J. Harries, J. Lowy, G. R. Mant, A. Svensson, and E. Towns-Andrews. 1994. Time-resolved x-ray diffraction studies of myosin head movements in live frog sartorius muscle during isometric and isotonic contractions. *J. Muscle Res. Cell Motil.* 15:319–348.

Matsubara, I., and G. F. Elliott. 1972. X-ray diffraction studies on skinned single fibers of frog skeletal muscle. *J. Mol. Biol.* 72:657–669.

Matsubara, I., Y. E. Goldman, and R. M. Simmons. 1984. Changes in the lateral filament spacing of skinned muscle fibers when cross-bridges attach. *J. Mol. Biol.* 173:15–33.

Maughan, D. W., and R. E. Godt. 1980. A quantitative analysis of elastic, entropic, electrostatic and osmotic forces within relaxed skinned muscle fibers. *Biophys. Struct. Mech.* 7:17–40.

Maughan, D. W., and R. E. Godt. 1981. Radial forces within muscle fibers in rigor. *J. Gen. Physiol.* 54:49–64.

Millman, B. 1998. The filament lattice of striated muscle. *Physiol. Rev.* 78:359–391.

Molloy, J. E., J. E. Burns, J. Kendrick-Jones, R. T. Tregear, and D. C. White. 1995. Movement and force produced by a single myosin head. *Nature.* 378:209–212.

Perrin, D. D., and I. G. Sayce. 1967. Computer calculation of equilibrium concentrations in mixtures of metal ions and complexing species. *Talanta.* 14:833–842.

Podolsky, R. J., H. St.-Onge, L. C. Yu, and R. W. Lymn. 1976. X-ray diffraction of actively shortening muscle. *Proc. Natl. Acad. Sci. U.S.A.* 73:813–817.

Poole, K. J. V., J. H. Kaplan, Y. Maédà, G. Rapp, and R. Goody. 1989. Dynamic tension and x-ray measurements on activation of rabbit psoas muscle using caged-calcium. *Biophys. J.* 55:12a.

Press, W. H., B. P. Flannery, S. A. Teukolsky, and W. T. Vetterling. 1989. Numerical Recipes: The Art of Scientific Computing. Cambridge University Press, Cambridge, UK.

Rapp, G., C. C. Ashley, M. A. Bagni, P. J. Griffiths, and G. Cecchi. 1998. Volume changes of the myosin lattice resulting from repetitive stimulation of single muscle fibers. *Biophys. J.* 75:2984–2995.

Tokunaga, M., K. Sutoh, C. Toyoshima, and T. Wakabayashi. 1987. Localisation of the ATPase site of myosin determined by three-dimensional electron microscopy. *Nature.* 329:635–638.

Vainshtein, B. K. 1966. Diffraction of X-Rays by Chain Molecules. Elsevier, Amsterdam.

Xu, S., B. Brenner, and L. C. Yu. 1993. State-dependent radial elasticity of attached cross-bridges in single skinned fibers of rabbit psoas muscle. *J. Physiol.* 465:749–765.

Yagi, N., S. Takemori, and M. Watanabe. 1993a. An x-ray diffraction study of frog skeletal muscle during shortening near the maximum velocity. *J. Mol. Biol.* 231:668–677.

Yagi, N., S. Takemori, and M. Watanabe. 1993b. Current x-ray diffraction experiments using a synchrotron radiation source. *Adv. Exp. Med. Biol.* 332:423–433.

Yagi, N., and S. Takemori. 1995. Structural changes in myosin cross-bridges during shortening of frog skeletal muscle. *J. Muscle Res. Cell Motil.* 16:57–63.

Yu, L. C., J. E. Hartt, and R. J. Podolsky. 1979. Equatorial x-ray intensities and isometric force levels in frog sartorius muscle. *J. Mol. Biol.* 132: 53–67.

Yu, L. C., A. C. Steven, G. R. S. Naylor, R. C. Gamble, and R. J. Podolsky. 1985. Distribution of mass in relaxed frog skeletal muscle and its redistribution upon activation. *Biophys. J.* 47:311–321.

Zite-Ferenczy, F., K. D. Haberle, R. Rüdel, and W. Wilke. 1986. Correlation between the light diffraction pattern and the structure of a muscle fiber realized with Ewald's construction. *J. Muscle Res. Cell Motil.* 7:197–214.